Available online at www.sciencedirect.com
ScienceDirect
Trans. Nonferrous Met. Soc. China 29(2019) 641−649
Transactions of Nonferrous Metals Society of China
www.tnmsc.cn

Recovery of valuable metals from lepidolite by atmosphere leaching and kinetics on dissolution of lithium

Jin-lian LIU[1, 2], Zhou-lan YIN[1], Xin-hai LI[3], Qi-yang HU[3], Wei LIU[1]

1. School of Chemistry and Chemical Engineering, Central South University, Changsha 410083, China;
2. Jiangxi Yunwei New Material Company Limited, Yichun 336000, China;
3. School of Metallurgy and Environment, Central South University, Changsha 410083, China

Received 8 December 2017; accepted 16 November 2018

Abstract: The lepidolite located in Yichun, Jiangxi Province, China, was adopted to investigate the recovery of alkali metals and leaching kinetics of lithium with sulphuric acid solution under atmospheric pressure. The results show that the recoveries of alkali metals were achieved under the leaching conditions: mass ratio of lepidolite with particle size less than 180 μm to sulphuric acid 1.2, leaching temperature 411 K, liquid−solid ratio 2.5:1, and leaching time 10 h. Under the selected conditions for leaching experiment, the leaching rates of lithium, potassium, rubidium and caesium are 94.18%, 93.70%, 91.81% and 89.22%, respectively. The X-ray diffraction analysis for leaching residue indicates that no insoluble product forms during leaching. The chemical compositions of leaching residue reveal that trace iron, manganese and calcium disappear after acid leaching. The kinetics of leaching process for lithium follows shrinking core model of mixed control and the apparent activation energy is 17.21 kJ/mol. The reaction orders with respect to sulphuric acid concentration and liquid−solid ratio are determined to be 2.85 and 1.66, respectively. A semi-empirical rate equation was obtained to describe the leaching process. The kinetic analysis shows that the leaching process is controlled by diffusion through the insoluble layer of the associated minerals.

Key words: kinetics; lepidolite; lithium; activation energy; leaching

1 Introduction

Lithium is widely utilized in battery industry and many other commercial products due to its fascinating electrochemical reactivity as well as other unique properties. Lithium chemicals and minerals find extensive applications in many industrial branches, such as ceramic, rubber, glass, aluminium, lubrication industries, metallurgical and pharmaceutical industries as raw materials [1,2]. It was reported that the use of lithium for batteries and related products has been increased by more than about 25% per year during the past several years. Prediction indicates that the total world lithium consumption is expected to increase by approximately 60% from 192000 t to 307000 t of lithium carbonate in the next 5 years, with the use of batteries in upcoming electric and hybrid vehicles taking a tremendous percentage (40000 t) of this growth [3,4].

Currently, majority of lithium products are extracted from the primary source of surface brines in the world, which typically contains 0.06%−0.15% Li due to the lower production costs compared with processing cost from lithium ores [5,6]. With the tremendous growth in demand for lithium and price rise, many potential ore deposits are being considered or have been developed to process lithium carbonate such as spodumene $LiAlSi_2O_6$ (6.0%−7.5%), petalite $LiAlSi_4O_{10}$ (3.5%−4.5%), lepidolite $K(Li,Al)_3(Al,Si)_4O_{10}(F,OH)_2$ (3.3%−7.74%), zinnwaldite $K(Li,Al,Fe)_3(Al,Si)_4O_{10}F_2$ (2%−5%) and also other solid minerals [1−7]. Spodumene is the purest form of those minerals containing Al and Si while petalite has higher Si content. Lepidolite and zinnwaldite contain Al in the same lattice with Li or Fe and also contain increased contents of valuable metals, such as Rb and Cs. Up to now, Rb is usually separated from the processing of lepidolite to extract lithium because of no minerals of its own [8−10].

Foundation item: Project (2015BAB06B01) supported by the National Key Technology R&D Program of China; Project (2014CB643406) supported by the National Basic Research Program of China
Corresponding author: Zhou-lan YIN; E-mail: yzllxh@gmail.com
DOI: 10.1016/S1003-6326(19)64974-5

Several methods have been developed to obtain lithium from all solid lithium minerals. Partial processes used in the below mentioned reports are subjected to a two-stage (roasting and leaching) treatment with aggressive media such as sulphuric acid, hydrochloric acid, lime, sodium and potassium salts and calcium sulphate at elevated temperature to obtain a water-soluble lithium salt [11,12]. However, the leaching process of lithium with pyrometallurgical methods consumed a large amount of energy, and SO_2 emission has received considerable attention due to more stringent environmental restrictions. These drawbacks of the roasting process limit their applications worldwide. Acid leaching is suitable for the recovery of valuable metals from complexes, especially low-grade ores with high contents of Si and waste rocks tailings [13−15]. The main advantage of the acid leaching is that the production of SO_2 can be avoided during the leaching process compared with the conventional method.

For the production of lithium carbonate from lithium minerals, two main alternatives have been proposed in recent years, including roasting leaching (RL) and acid leaching (AL) directly [16,17]. Compared with the AL process, the RL process has a shorter roasting and leaching time. CHEN et al [18] reported that the α-spodumene was roasted at elevated temperature of 1323 K for 30 min for crystal transformation and then leached for 120 min to ensure lithium salts into the lixivium more efficiently. The leaching of lithium from granite by using sulphuric acid was carried out in an autoclave above 533 K [19]. The acid-roasting method applied in lithium ores such as spodumene has been reported during the past years [20].

The effects of heat treatment on the lithium leaching rate have been intensively studied [21]. However, there is a lack of detailed investigation about kinetic of lithium recovery from lepidolite. Despite the hydrometallurgical process has emerged as a promising technology for lithium leaching from lepidolite, it has not been commercialized worldwide. Leaching of lithium in sulphuric acid is complicated and it is not surprising that the reaction kinetic for the system has not been reported [22].

The purpose of the present research is to recommend results on the characterization and leaching of lepidolite by diluted sulphuric acid. The factors studied were temperature, reaction time, acid concentration, liquid−solid (L/S) ratio and particle size. Through analysis of the above factors, we established the controlling kinetic model of the reaction process. This model can provide a scientific approach and a theoretic basis for the mechanisms of leaching lithium from lepidolite at optimal performance and reagent consumption. The X-ray diffraction (XRD) measurement and inductively coupled plasma atomic emission spectroscopy (ICP−AES) method were also used to interpret the results of leaching experiments.

2 Experimental

2.1 Materials

The lepidolite was provided by Jiangxi Province of China. It was ground in a ball mill and sieved to less than 180 μm before it was used as the samples for the leaching tests. The chemical composition of the lepidolite is listed in Table 1 and the XRD pattern is shown in Fig. 1. The lepidolite sample that can be used in this investigation is a fairly pure crystal as indicated by 2.12% Li, 1.25% Na, 6.50% K, 1.21% Rb, 0.20% Cs, 14.26% Al, 4.46% F, 50.78% SiO_2 and containing 0.24% Mn, 0.14% Ca, 0.13% Fe as impurities. The raw material contains primarily lepidolite ($K(Li,Al)_3(Si,Al)_4O_{10}$-$(F,OH)_2$), albite ($NaAlSi_3O_8$) and quartz ($SiO_2$). All chemicals used in the experiments are analytical grade reagents. Deionized water was used to prepare solutions for the experimental procedures and also for all the analytical tests.

Table 1 Chemical composition of raw ore (mass fraction, %)

Li	Na	K	Rb	Cs	SiO_2
2.12	1.25	6.50	1.21	0.20	50.78
Al	F	Fe	Mn	Ca	
14.26	4.46	0.13	0.24	0.14	

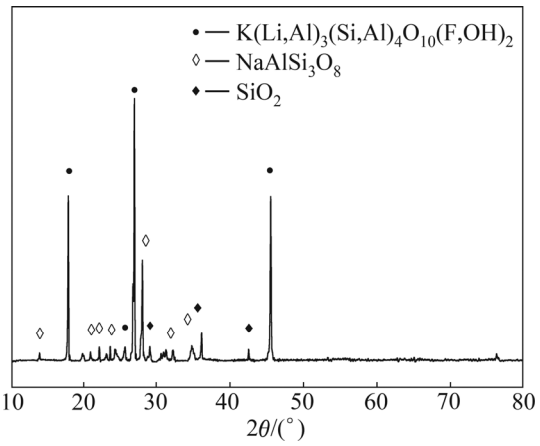

Fig. 1 XRD pattern of lepidolite

2.2 Experimental process

The leaching experiments were implemented in a 1000 mL three-neck flask glass reactor connected with a condenser pipe and agitated by a mechanical stirrer. The reaction temperature was maintained to be constant in an oil bath heated by an electric heater. All the experiments were conducted in batches with 200 g lepidolite. Firstly, a specific amount of diluted sulphuric acid solution was

added into the reactor. The solution was heated up to a specified temperature under stirring. Up to temperature stabilization, a certain amount of lepidolite was added into sulphuric acid solution to initiate the reaction. 2 mL of sample solution was withdrawn from leaching solution at specific time and filtered for analyzing the concentrations of all valuable metals. After reaction, the slurry was separated by vacuum filtration and the leaching residue was dried in an oven at 313 K.

2.3 Analytical methods

The leaching process was followed by sampling of solution at a chosen time interval, and then measured the concentrations of Li, K, Rb and Cs by an ICP−AES method. Fluorine and aluminum were determined with a fluoride ion selective electrode and titration, respectively. Fluoride and aluminium were determined three times to obtain the average values. Relative standard deviations were found to be within ±0.5%. The leaching rates of valuable metals were calculated using the following volume correct formula [23]:

$$X_i = \frac{(V_0 - \sum_{i=1}^{i-1} V_i)c_{\mathrm{Li},i} + \sum_{i=1}^{i-1} V_i c_{\mathrm{Li},i}}{m\frac{c_{\mathrm{Li}}}{100}} \quad (1)$$

where V_0 is the initial volume of the leaching solution (mL), V_i is the volume of the sample solution i (mL), c_{Li} is the content of lithium in the lepidolite (mass fraction, %, dried solid), $c_{\mathrm{Li},i}$ is the concentration of lithium in sample i (g/L), and m is the initial mass of lepidolite (g, dried solid).

3 Results and discussion

3.1 Chemical reactions during process leaching

Up to now, the mechanism of reduction dissolution for lepidolite in sulphuric acid solution remains unclear. The lepidolite is only partially dissolved and reacted with sulphuric acid to form alkali metal sulphate and aluminium sulphate during acid leaching, and the amounts of alkali metals and aluminium in the residue are very low. Only a trace of Fe and Mn in the minerals are dissolved into the leaching solution, which have little influence on the acid consumption, leaching rates of all valuable metals, lithium concentration in leaching solution and the product composition. The effect of the recovery of lithium on the leaching kinetic plays a significant role in the following discussion. The main chemical reactions during leaching may be expressed as follows:

$$Me_2O(s)+H_2SO_4(aq)=Me_2SO_4(aq)+H_2O \quad (2)$$

where Me are alkali metals, which can react with sulphuric, chlorine and nitric acids.

Aluminium, iron, manganese and calcium exist in lithium minerals of lepidolite. They will also react with sulphuric acid in the leaching solution, and the reactions are as follows:

$$Al_2O_3(s)+3H_2SO_4(aq)=Al_2(SO_4)_3(aq)+3H_2O \quad (3)$$

$$FeO, MnO, CaO(s)+3H_2SO_4(aq)= (Fe,Mn)SO_4(aq)+CaSO_4(s)+3H_2O \quad (4)$$

The most common process involves the leaching of mixed alkali metals from the original minerals by prolonged leaching time, and mixed alums are developed by reacting an aqueous solution of aluminium sulphate and the corresponding Me_2SO_4 includes potassium, rubidium and caesium sulphates in a stoichiometric proportion partially, and then all the soluble mixed alums decrease with the increased atomic number [24].

$$Me_2SO_4(aq)+Al_2(SO)_3(aq)+24H_2O= 2MeAl(SO_4)_2\cdot 12H_2O(aq) \quad (5)$$

Therefore, at the end of dissolution reaction, the leaching residue consists mainly of quartz and albite. All metallic elements are dissolved to form metallic sulphate and mixed alums in the solution.

3.2 Effect of experimental parameters on leaching process

As valuable metals and silica exist predominantly in the lepidolite, all alkali metals, aluminium and trace of iron, manganese, will dissolve into the leaching solution, and thus the leaching rates of these metals will reflect the leaching extent of lepidolite.

3.2.1 Effect of initial acid concentration

The effects of initial acid concentration on the leaching rates of alkali metals and aluminium were studied by varying mass ratio of acid to lepidolite over the range of 0.6:1−1.6:1, maintaining the reaction temperature at 411 K, 2.5:1 of L/S ratio, particle size less than 180 μm and 10 h of reaction time.

As can be seen in Fig. 2, when the mass ratio of acid to lepidolite is no more than 0.8:1, the leaching rates of alkali metals are less than 70%, which is due to lack of sulphuric acid in the slurry. When the mass ratio increases from 0.8:1 to 1.2:1, the leaching rate of lithium increases significantly. The lithium leaching rate improves from 92.71% to 97.99% when the mass ratio increases from 1.2:1 to 1.6:1. The leaching rate improvements of alkali metals and aluminium are probably due to the increase of H^+ activity that will result in subsequent reaction of valuable metals in the residue. But higher mass ratio will increase the consumption of H_2SO_4 and reduce the concentration of valuable metals in the resultant solution. Therefore, a mass ratio of 1.2:1 is employed in order to optimize the leaching process.

3.2.2 Effect of L/S ratio

The effects of L/S ratio in the range from 1.5:1 to

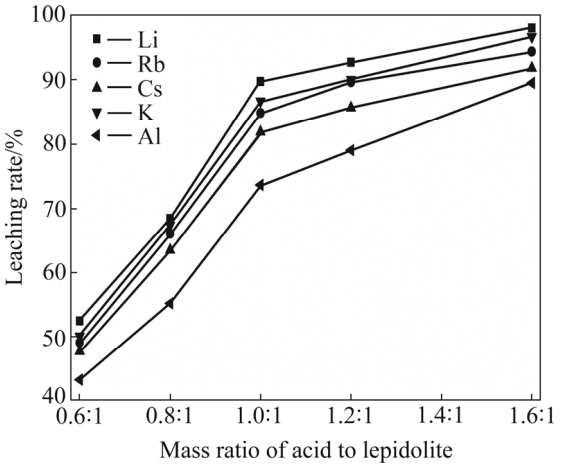

Fig. 2 Effect of initial acid concentration on leaching rates of valuable metals (411 K, L/S ratio 2.5:1, particle size less than 180 μm)

4:1 on the leaching rates of valuable metals were studied, maintaining the mass ratio of acid to lepidolite at 1.2:1, reaction temperature at 411 K, particle size less than 180 μm and 10 h of reaction time.

As can be seen in Fig. 3, increasing the L/S ratio from 1.5:1 to 3:1, an obvious increase in the leaching rate of alkali metals is obtained. The leaching rate increases from 80.08% to 92.72% for lithium and from 77.11% to 87.37% for other alkali metals, with the increase of L/S ratio from 1.5:1 to 2.5:1, while the recovery of aluminium increases by about 13.12%. When L/S ratio of 4:1 is used, a lithium leaching rate of 97.75% can be obtained, as can be expected, a further increase in L/S ratio from 2.5:1 to 4.0:1 has little impact on the leaching rates of alkali metals. Therefore, the L/S ratio is kept constant at 2.5:1 for the subsequent experiments.

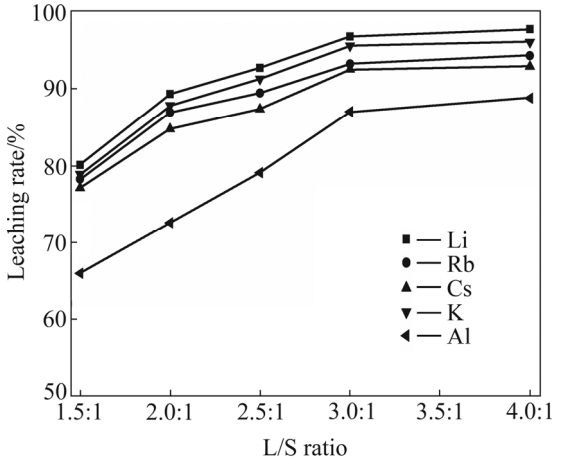

Fig. 3 Effect of L/S ratio on leaching rates of valuable metals (411 K, initial acid concentration 50%, particle size less than 180 μm)

3.2.3 Effect of temperature

The effects of reaction temperature on the leaching rates of alkali metals and aluminium were investigated in the temperature range of 351 to 421 K. During these experiments, the L/S ratio was maintained to be 2.5:1, the mass ratio of acid to lepidolite was 1.2:1, particle size was less than 180 μm and reaction time was 10 h.

The results are shown in Fig. 4. It can be seen that the leaching rates of valuable metals increase with increasing temperature, alkali metals are readily leached at 351 K or lower temperatures. With the increase in the reaction temperature from 351 to 411 K, lithium leaching rate increases from 59.13% to 94.18%. The economical leaching rates of potassium, rubidium and caesium are 93.70%, 91.81% and 89.22% when the temperature is 411 K, respectively, and the leaching rates of all other alkali metals are lower than that of lithium. Also, it is clear that the maximum leaching rate of aluminium is 82.63% at 411 K, and then decreases with further increasing temperature. The low dissolution of aluminium at higher temperature is probably due to precipitation of Al−F complexes. The fact that the leaching rates of alkali metals and aluminium increase with the temperature increasing may be attributed to the intensive diffusivity of sulphate.

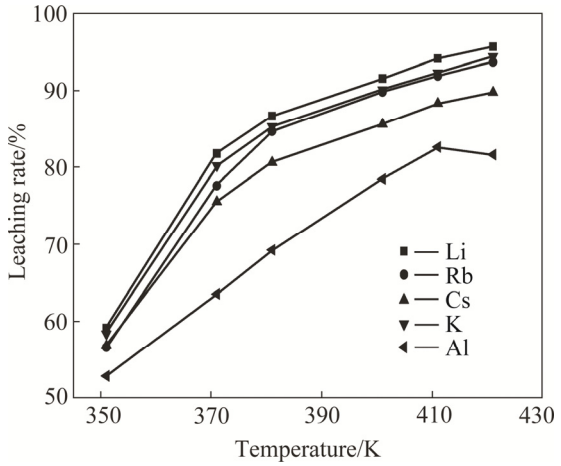

Fig. 4 Effect of temperature on leaching rates of valuable metals (L/S ratio 2.5:1, initial acid concentration 50%, particle size less than 180 μm)

3.2.4 Effect of particle size

The effects of particle size on the leaching rates of alkali metals were studied. These experiments were conducted at 411 K, mass ratio of acid to lepidolite 1.2:1, L/S ratio 2.5:1 and reaction time 10 h. As shown in Fig. 5, the leaching rate of lithium increases with the particle size decreasing, but the particle size plays a minor role in the leaching process. The maximum leaching rate of lithium reaches 85.89% when the particle size is above 380 μm, whereas 95.12% lithium is extracted when the particle size is less than 96 μm. The leaching rates of other alkali metals are presented in Table 2. The results show that the leaching rate of

lithium is the highest, and that of caesium is the lowest of all the alkali metals. The leaching rates of alkali metals are both up to 88.86% when the particle size is 96−180 μm. The leaching rates of alkali metals increase gradually and then keep almost constant with the decrease of particle size. It is necessary to grind the lepidolite and sieve to less than 180 μm before leaching in order to improve leaching efficiency.

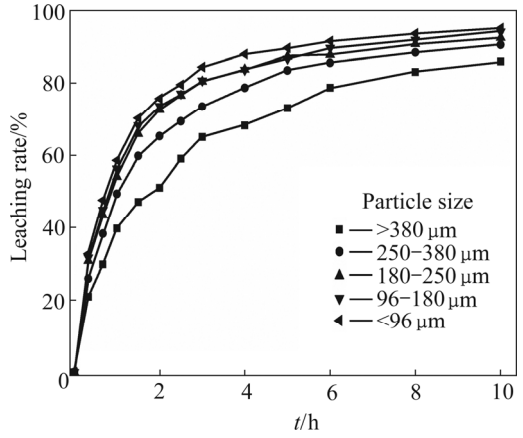

Fig. 5 Effect of particle size on leaching rate of lithium (411 K, L/S ratio 2.5:1, initial acid concentration 50%)

Table 2 Effect of particle size on leaching rate of all elements

Particle size/μm	Leaching rate/%			
	Lithium	Potassium	Rubidium	Caesium
>380	85.89	84.90	81.75	77.11
250−380	90.55	89.40	85.65	84.78
180−250	92.5	91.69	86.86	85.37
96−180	94.14	92.47	88.86	96.55
<96	95.13	93.44	90.04	98.93

3.3 Morphology of leaching residue

The mineralogical composition of the lepidolite after sulphuric acid leaching was examined by XRD. The corresponding XRD pattern in Fig. 6 shows that the primary phases of leaching residue are albite ($NaAlSi_3O_8$) and quartz (SiO_2).

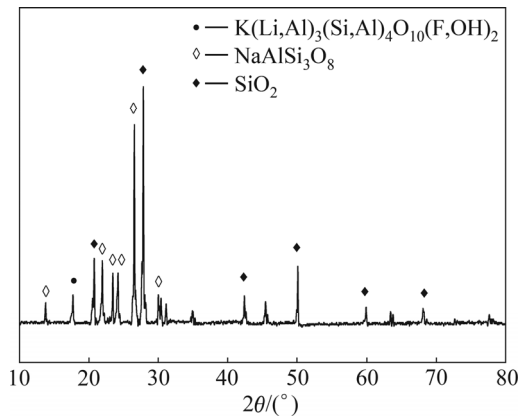

Fig. 6 XRD pattern of leaching residue

The chemical compositions of leaching residue are listed in Table 3. The results indicate that alkali metals and trace amount of Fe, Mn and Ca disappear after the leaching experiments. These results suggest that no insoluble product forms during the leaching processes.

Table 3 Chemical composition of residue (mass fraction, %)

Li	Na	K	Rb	SiO_2	Al	F
0.12	0.85	0.28	0.01	50.78	3.07	1.85

3.4 Kinetic analysis

Kinetic modelling yields comprehensive information regarding leaching mechanisms. In a fluid−solid reaction system, if the mixed lepidolite ore particles are considered as nonporous particles, and the ore grains gradually shrank and the product layers form around the unreacted grains during the leaching process of alkali metals. The heterogeneous non-catalytic reaction for lepidolite may be kinetically interpreted by using the shrinking core model (SCM) while other models such as homogeneous, grain and pore models are usually applied to the porous solid−liqiud system [25−27].

Figure 5 indicates that the diffusion through the liquid film surrounding a solid particle does not act as a rate-controlling step under the particle size less than 96 μm. Therefore, only diffusion through the product layer and chemical reaction on the surface of the unreacted core should be carefully considered when discussing the controlling step. According to Eq. (2), the leaching reactions are irreversible reactions, and the leaching process can be described as two independent models, based on the SCM of which liquid film diffusion control is neglected.

Assuming that lepidolite has a spherical geometry and the process is controlled by the surface chemical reaction, the integrated equation of the shrinking core model can be given as follows [28]:

$$\begin{cases} 1-(1-x)^{1/3}=k_{\mathrm{r}}t \\ k_{\mathrm{r}}=\dfrac{kM_{\mathrm{s}}}{a\rho_{\mathrm{s}}r_0}c_{\mathrm{A}} \end{cases} \tag{6}$$

where x is the lithium leaching rate, t is real leaching time, k_{r} is the apparent rate constant calculated from Eq. (6), k is the kinetic constant, M_{s} is the relative molecular mass of solid, c_{A} is the acid concentration, a is the stoichiometric coefficient of reagent in reaction, ρ_{s} is the density of the solid, and r_0 is the initial radius of particle.

Similarly, if the leaching products form on the surface of the unreacted grains and the volume of products is the same as that of the reacted solids, the particle size will keep constant and the radius of the particle is equal to r_0 during leaching [26]. If sulphuric

acid concentration is constant during leaching, the rate of reaction can be expressed as

$$\begin{cases} 1-\dfrac{2}{3}x-(1-x)^{2/3}=k_{\mathrm{d}}t \\ k_{\mathrm{d}}=\dfrac{2M_{\mathrm{s}}D_{\mathrm{Aeff}}}{a\rho_{\mathrm{s}}r_0^2}c_{\mathrm{A}} \end{cases} \tag{7}$$

where D_{Aeff} is the diffusion coefficient in porous product layer.

According to Eqs. (6) and (7), when the chemical reaction and outer diffusion are the rate controlling step, a plot of $1-(1-x)^{1/3}$ vs time is a straight line with a slope of k_{r}. On the contrary, when the leaching process is controlled by inner diffusion through the solid product layer, a plot of $1-(2/3)x-(1-x)^{2/3}$ vs time is a straight line with a slope of k_{d} [28,29]. Equations (6) and (7) are often used to describe the process when it is controlled by chemical reaction or diffusion in nonporous liquid−solid system.

3.5 Empirical kinetic equation

In order to determine the controlling step and carry out kinetic analysis in this work, the SCMs with surface chemical reaction and diffusion through product layer, Eqs. (6) and (7) were evaluated. The left sides of these expressions are plotted with respect to the leaching time and then the dependency models on the kinetic data are evaluated with correlation coefficient (R^2) values. The slops of these plots are the apparent rate constants (k_{r} and k_{d}).

Experimental data were substituted into Eqs. (6) and (7), and correlation coefficient (R^2) were calculated, as given in Table 4. The results indicate that the dissolution controlled model (Eq. (7)) is fitted with the data better in the range of experiments and the correlation coefficients (R^2) are greater than 0.96. Figure 7 shows the good fitting obtained by plotting $1-(2/3)x-(1-x)^{2/3}$ vs time at different temperatures. In addition, the type of reaction does not confirm to surface chemical reaction and the correlation coefficients (R^2) are lower than 0.96. It is then illustrated that the kinetic data are fitted with the shrinking core model, in which the leaching process is controlled by diffusion through the insoluble layer of the associated minerals.

Table 4 Correlation coefficient (R^2) of two kinetic models at different temperatures

T/K	R^2	
	$1-(1-x)^{1/3}$	$1-(2/3)x-(1-x)^{2/3}$
351	0.9496	0.9910
371	0.9654	0.9907
381	0.8784	0.9959
401	0.8403	0.9943
411	0.9333	0.9637
421	0.9137	0.9983

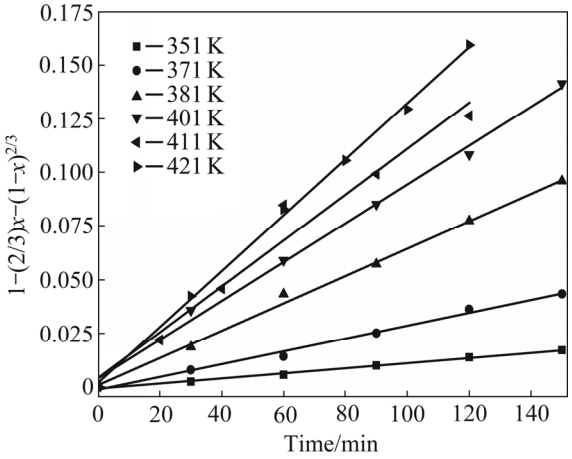

Fig. 7 Plots of $1-(2/3)x-(1-x)^{2/3}$ vs time at different temperatures (L/S ratio 2.5:1, initial acid concentration 50%, particle size less than 180 μm)

The apparent activation energy E_{a} was determined based on the Arrhenius equation:

$$\ln k_{\mathrm{d}}=\ln A-\frac{E_{\mathrm{a}}}{RT} \tag{8}$$

where A is the pre-exponential factor. Arrhenius plot of $\ln k_{\mathrm{d}}$ vs T^{-1} for lithium leaching data is shown in Fig. 8. The apparent activation energy calculated from the slope of the line is 17.21 kJ/mol at 351−421 K.

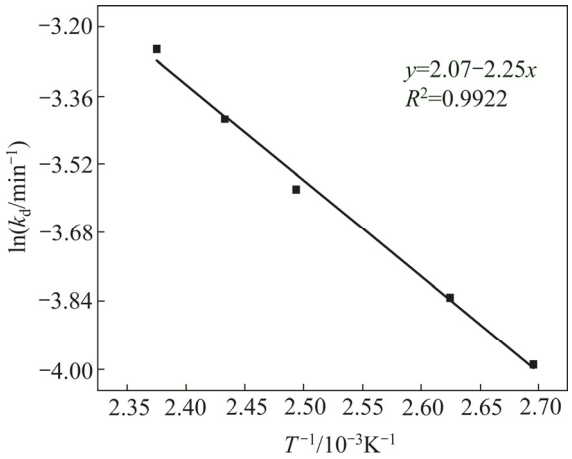

Fig. 8 Arrhenius plot for lithium dissolution from lepidolite

A similar fitting plot of $1-(2/3)x-(1-x)^{2/3}$ vs time was obtained at initial different sulphuric acid concentrations c_0 and shown in Fig. 9(a). From the slopes of the straight lines shown in Fig. 9(b), the apparent rate constant (k_{d}) values were determined and a plot of $\ln k_{\mathrm{d}}$ vs $\ln c_0$ was obtained to determine the order of dependency with respect to the concentration of sulphuric acid. The reaction order with respect to the concentration of sulphuric acid is 2.85.

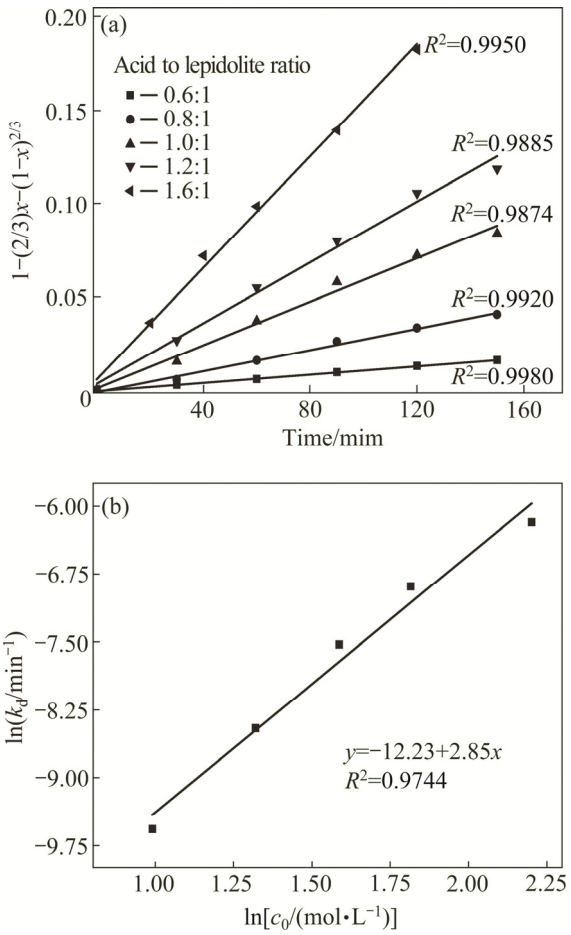

Fig. 9 Fitting of experimental data according to Eq. (7) at different initial acid concentrations (L/S ratio 2.5:1, 411 K, particle size less than 180 μm): (a) $1-(2/3)x-(1-x)^{2/3}$ vs time; (b) $\ln k_d$ vs $\lg c_0$

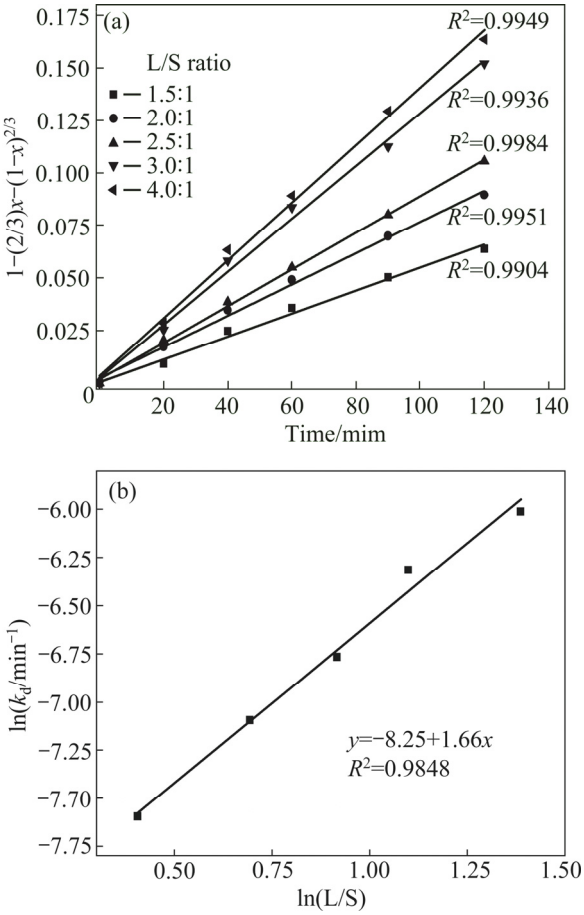

Fig. 10 Fitting of experimental data according to Eq. (7) at different L/S ratios (initial acid concentration 50%, 411 K, particle size less than 180 μm): (a) $1-(2/3)x-(1-x)^{2/3}$ vs time; (b) $\ln k_d$ vs ln(L/S)

Similarly, the straight lines of $1-(2/3)x-(1-x)^{2/3}$ vs time were obtained at different L/S ratios and shown in Fig. 10(a). The experimental k_d values were determined and $\ln k_d$ vs ln(L/S) plot is shown in Fig. 10(b). It is calculated that the reaction rate is proportional to the power of 1.66 for L/S ratio.

The control factors of leaching temperature, sulphuric acid concentration and L/S ratio were applied to developing the kinetic model. According to the above results and Eq. (7), the apparent rate constant k_d can be expressed as follows:

$$k_d = \frac{k_0}{r_0^2} c_0^{2.85} r_{L/S}^{1.66} \exp[-17210/(RT)] \quad (9)$$

By the above analysis, comparing Eq. (7) with Eq. (9), the kinetic model of lepidolite leaching by H_2SO_4 can be described as follows:

$$1-\frac{2}{3}x-(1-x)^{2/3} = \frac{k_0}{r_0^2} c_0^{2.85} r_{L/S}^{1.66} \exp[-17210/(RT)]t \quad (10)$$

The value of k_0 can be calculated from the straight line in Fig. 7 to be 1.18. Consequently, Eq. (11) can be described as the kinetic expression to interpret the dissolution of lithium from lepidolite in sulphuric acid solutions.

$$1-\frac{2}{3}x-(1-x)^{2/3} = \frac{1.18}{r_0^2} c_0^{2.85} r_{L/S}^{1.66} \exp[-17210/(RT)]t \quad (11)$$

4 Conclusions

(1) The recovery of alkali metals from lepidolite and the leaching kinetics of lithium were investigated in sulphuric acid at atmospheric pressure. The results show that the recoveries of alkali metals were achieved under the leaching conditions: mass ratio of acid to lepidolite 1.2:1, leaching temperature 411 K, L/S ratio 2.5:1, particle size less than 180 μm and leaching time 10 h. Under the selected conditions for leaching experiment, the leaching rates of lithium, potassium, rubidium and caesium are 94.18%, 93.70%, 91.81% and 89.22%,

respectively.

(2) The X-ray diffraction analysis indicates that no insoluble product forms during the leaching process, the chemical compositions of leaching residue show that alkali metals can be dissolved and trace amount of Fe, Mn and Ca disappear after the leaching experiments.

(3) The leaching process follows the kinetics of a shrinking core model and the apparent activation energy is 17.21 kJ/mol. The kinetics expression to interpret the dissolution of lithium from lepidolite in sulphuric acid solutions is obtained.

References

[1] MARTIN G, SCHNEIDER A, VOIGT W, BERTAU M. Lithium extraction from the mineral zinnwaldite. Part II: Lithium carbonate recovery by direct carbonation of sintered zinnwaldite concentrate [J]. Minerals Engineering, 2017, 110(15): 75−81.

[2] ROSALES G D, RUIZ M C, RODRIGUEZ M H. Novel process for the extraction of lithium from β-spodumene by leaching with HF [J]. Hydrometallurgy, 2014, 147−148: 1−6.

[3] VIECELI N, NOGUEIRA C A, PEREIRA M F, DURAO F O, GUIMARAESC C, MARGARIDO F. Recovery of lithium carbonate by acid digestion and hydrometallurgical processing from mechanically activated lepidolite [J]. Hydrometallurgy, 2018, 175: 1−10.

[4] LUONG V T, KANG D J, AN J W, DAO D A, KIM M J, TRAN T. Iron sulphate roasting for extraction of lithium from lepidolite [J]. Hydrometallurgy, 2014, 141: 8−16.

[5] ZHU Cheng-cai, DONG Ya-ping, YUN Zeng, HAO Yong, WANG Chun, DONG Nai-jin, LI Wu. Study of lithium exploitation from carbonate subtype and sulfate type salt-lakes of Tibet [J]. Hydrometallurgy, 2014, 149: 143−147.

[6] LI Yan-hong, ZHAO Zhong-wei, LIU Xu-heng, CHEN Xing-yu, ZHONG Mao-li. Extraction of lithium from salt lake brine by aluminum-based alloys [J]. Transactions of Nonferrous Metals Society of China, 2015, 25: 3484−3489.

[7] BARBOSA L I, GONZALEZ J A, RUIZ M C. Extraction of lithium from β-spodumene using chlorination roasting with calcium chloride [J]. Thermochimica Acta, 2015, 605: 63−67.

[8] AYLMOREA M G, MERIGOT K, RICKARD W D, EVANS N J, MCDONALD B J, CATOVIC E, SPITALNY P. Assessment of a spodumene ore by advanced analytical and mass spectrometry techniques to determine its amenability to processing for the extraction of lithium [J]. Minerals Engineering, 2018, 119: 137−148.

[9] SITANDO O, CROUSE P L. Processing of a Zimbabwean petalite to obtain lithium carbonate [J]. International Journal of Mineral Processing, 2012, 102: 45−50.

[10] CHOUBEY P K, KIM M S, SRIVASTAVA R R, LEE J C, LEE J Y. Advance review on the exploitation of the prominent energy-storage element: Lithium. Part I: From mineral and brine resources [J]. Minerals Engineering, 2016, 89: 119−137.

[11] YAN Qun-xuan, LI Xin-hai, WANG Zhi-xing, WU Xi-fei, GUO Hua-jun, HU Qi-yang, PENG Wen-jie, WANG Jie-xi. Extraction of valuable metals from lepidolite [J]. Hydrometallurgy, 2012, 117: 116−118.

[12] HIEN-DINH T T, LUONG V T, GIERE R, TRAN T. Extraction of lithium from lepidolite via iron sulphide roasting and water leaching [J]. Hydrometallurgy, 2015, 153: 154−159.

[13] LIU Zhi-xiong, YIN Zhou-lan, HU Hui-ping, CHEN Qi-yuan. Leaching kinetics of low-grade copper ore containing calcium−magnesium carbonate in ammonia−ammonium sulfate solution with persulfate [J]. Transactions of Nonferrous Metals Society of China, 2012, 22: 2822−2830.

[14] LAJOIE-LEROUX F, DESSEMOND C, SOUCY G, LAROCHE N, MAGNAN J F. Impact of the impurities on lithium extraction from β-spodumene in the sulfuric acid process [J]. Minerals Engineering, 2018, 129: 1−8.

[15] KUANG Ge, LIU Yu, LI Huan, XING Sheng-zhou, LI Fu-jie, GUO Hui. Extraction of lithium from β-spodumene using sodium sulfate solution [J]. Hydrometallurgy, 2018, 177: 49−56.

[16] YAN Qun-xuan, LI Xin-hai, WANG Zhi-xing, WANG Jie-xi, GUO Hua-jun, HU Qi-yang, PENG Wen-jie, WU Xi-fei. Extraction of lithium from lepidolite using chlorination roasting water leaching process [J]. Transactions of Nonferrous Metals Society of China, 2012, 22: 1753−1759.

[17] KUANG Ge, LI Huan, HU Song, JIN Ran, LIU Shan-jun, GUO Hui. Recovery of aluminium and lithium from gypsum residue obtained in the process of lithium extraction from lepidolite [J]. Hydrometallurgy, 2015, 157: 214−218.

[18] CHEN Ya, TIAN Qian-qiu, CHEN Bai-zhen, SHI Xi-chang, LIAO Ting. Preparation of lithium carbonate from spodumene by a sodium carbonate autoclave process [J]. Hydrometallurgy, 2011, 109: 43−46.

[19] DISTIN P A, PHLLIPS C V. The acid extraction of lithium from the granites of South West England [J]. Hydrometallurgy, 1982, 9(1): 1−14.

[20] BARBOSA L I, VALENTE G, OROSCO R P, GONZALEZ J A. Lithium extraction from β-spodumene through chlorination with chlorine gas [J]. Minerals Engineering, 2014, 56: 29−34.

[21] OGORODOVA L P, KISELEVA I A, MELCHAKOVA L V, SCHURIGA T N. Thermodynamic properties of lithium mica: Lepidolite [J]. Thermochimica Acta, 2005, 435: 68−70.

[22] YAN Qun-xuan, LI Xin-hai, YIN Zhou-lan, WANG Zhi-xing, GUO Hua-jun, PENG Wen-jie, HU Qi-yang. A novel process for extracting lithium from lepidolite [J]. Hydrometallurgy, 2012, 121: 54−59.

[23] LI Min-ting, WEI Chang, QIU Shuang, ZHOU Xue-jiao, LI Cun-xiong, DENG Zhi-gan. Kinetics of vanadium dissolution from black shale in pressure acid leaching [J].Hydrometallurgy 2010, 104: 193–200.

[24] NAIDU G, JEONG S, CHOI Y, SONG M H, OYUNCHULUUN U, VIGNESWARAN S. Valuable rubidium extraction from potassium reduced seawater brine [J]. Journal of Cleaner Production, 2018, 174: 1079−1088.

[25] LIU Kui, CHEN Qi-yuan, YIN Zhou-lan, HU Hui-ping, DING Zhi-ying. Kinetics of leaching of a Chinese laterite containing maghemite and magnetite in sulfuric acid solutions [J]. Hydrometallurgy, 2012, 125: 125−136.

[26] TIAN Jun, YIN Jing-qun, CHI Ru-an, RAO Guo-hua, JIANG Min-tao, OUYANG Ke-xian. Kinetics on leaching rare earth from the weathered crust elution-deposited rare earth ores with ammonium sulfate solution [J]. Hydrometallurgy, 2010, 101(3−4): 166−170.

[27] CHI Ru-an, ZHU Guo-cai, TIAN Jun. Leaching kinetics of rare earth from black weathering mud with hydrochloric acid [J]. Transactions of Nonferrous Metals Society of China, 2000, 10: 531−533.

[28] LIU Hui-bin, DU Hao, WANG Da-wei, WANG Shao-na, ZHENG Shi-li, ZHANG Yi. Kinetics analysis of decomposition of vanadium slag by KOH sub-molten salt method [J]. Transactions of Nonferrous Metals Society of China, 2013, 23: 1489−1500.

[29] ZHANG Xing-ran, LIU Zuo-hua, WU Xi-bin, DU Jun, TAO Chang-yuan. Electric field enhancement in leaching of manganese from low-grade manganese dioxide ore: Kinetics and mechanism study [J]. Journal of Electroanalytical Chemistry, 2017, 788: 165−174.

锂云母矿中有价金属的常压提取及锂的溶出动力学

刘金练[1,2]，尹周澜[1]，李新海[3]，胡启阳[3]，刘 伟[1]

1. 中南大学 化学化工学院，长沙 410083；2. 江西云威新材料矿业有限公司, 宜春 336000；
3. 中南大学 冶金与环境学院，长沙 410083

摘 要：研究产于江西省宜春市的锂云母矿在硫酸体系常压浸出过程中有价碱金属元素的提取，建立该反应过程中锂的溶出动力学方程。结果表明：在粒径小于 180 μm 物料与硫酸质量比为 1.2:1、温度为 411 K、液固比为 2.5:1 的条件下浸出 10 h，锂、钾、铷和铯的浸出率分别为 94.18%、93.70%、91.81%和 89.22%。浸出矿渣的 X 射线衍射分析结果表明，浸出过程中无不溶物产生，浸出渣化学组分表明矿相中微量的铁、锰、钙等随酸浸过程的进行逐步消失。锂的浸出动力学行为符合混合控制的收缩核模型，反应的表观活化能为 17.21 kJ/mol，硫酸浓度和液固比相应的反应级数分别为 2.85 和 1.66。得到半经验速率方程以描述整个浸出过程。动力学分析结果表 明，浸出过程由伴生矿物的不溶层扩散控制。

关键词：动力学；锂云母；锂；活化能；浸出

(Edited by Wei-ping CHEN)